

A thermodynamic model for hydrous silicate melts in the system NaAlSi3O8–KAlSi3O8–Si4O8–H2O

Marcus Kirschen, Michel Pichavant

▶ **To cite this version:**

Marcus Kirschen, Michel Pichavant. A thermodynamic model for hydrous silicate melts in the system NaAlSi3O8–KAlSi3O8–Si4O8–H2O. Chemical Geology, 2001, 174, pp.103-114. 10.1016/S0009-2541(00)00310-7 . hal-00089786

HAL Id: hal-00089786

https://insu.hal.science/hal-00089786

Submitted on 28 Aug 2006

HAL is a multi-disciplinary open access archive for the deposit and dissemination of scientific research documents, whether they are published or not. The documents may come from teaching and research institutions in France or abroad, or from public or private research centers.

L'archive ouverte pluridisciplinaire **HAL**, est destinée au dépôt et à la diffusion de documents scientifiques de niveau recherche, publiés ou non, émanant des établissements d'enseignement et de recherche français ou étrangers, des laboratoires publics ou privés.

A thermodynamic model for hydrous silicate melts in the system $NaAlSi_3O_8$–$KAlSi_3O_8$–Si_4O_8–H_2O

Marcus Kirschen' and Michel Pichavant

Centre National de Recherche Scientifique, Centre de Recherches sur la Synthèse et la Chimie des Minéraux CRSCM, 1A rue de la Férollerie, F-45071 Orléans Cedex 2, France – remplacé par UMR6113 - ISTO

Abstract

Computation of crystal–liquid equilibria in hydrous silicate systems requires a model of the free energy of the hydrous liquid that defines the activity of the melt components at given temperature, pressure and composition. We present in this study a parametrization of the free energy of the liquid in the haplogranite system $NaAlSi_3O_8$–$KAlSi_3O_8$–Si_4O_8–H_2O based on the Margules approach. The excess free energy of the multicomponent melt is approximated from the binaries with the Kohler extrapolation method. Model parameters have been fitted to phase equilibrium data by mathematical programming techniques. A small but complex excess function of the anhydrous melt composition is necessary to reproduce reported liquidus phase relations. Using partial molar C_p data from the literature for the H_2O melt component and a simple polynomial approximation for the molar volume, standard state enthalpy and entropy were refined close to −287 kJ/mol and 67.2 J/K mol, respectively. Calculated crystal–liquid phase relations are in good agreement with measurements to 5 kbar, and the modelled melt–fluid coexistence surface yields a valuable first order approximation of the H_2O solubility at near liquidus temperatures. Thermodynamic assessment of solubility and liquidus data suggests that H_2O mixing differs considerably in feldspar melts and in silica melts. Si_4O_8–H_2O mixing contributes to a very minor degree to the haplogranite system.

Author Keywords: Haplogranite system; Hydrous silicate melt; Liquidus phase equilibria; Linear programming

1. Introduction

The influence of H_2O on melting and crystallization temperatures of silicic magmas has been for decades an attractive research topic in geosciences since the pioneering studies from Goranson and Goranson, Bowen and Tuttle (1950) and Tuttle and Bowen (1958) at high pressures and under H_2O-saturated conditions. The haplogranite system $NaAlSi_3O_8$(ab)–$KAlSi_3O_8$(or)–Si_4O_8(qtz)–H_2O has been widely accepted as an analogue for a broad range of natural silicic magmas. More recently, liquidus phase equilibria were determined at high pressures and for H_2O-undersaturated conditions in order to distinguish the effects of pressure and H_2O activity on phase relations in the haplogranite system (Steiner, 1970; Fenn, 1973; Holtz; Pichavant and Becker). Analytical techniques were significantly improved, too, allowing the H_2O content of the quench glasses to be precisely measured by infrared spectroscopy and Karl Fischer titration (KFT) (e.g. Behrens and Behrens). This extensive experimental database provides an excellent tool to test and to develop existing thermodynamic models of hydrous silicate melts. Presently, few thermodynamic models exist for multicomponent hydrous silicate melts (e.g. Nekvasil; Blencoe; Ghiorso and Wen). The scope of the present study is the derivation of a thermodynamic model for hydrous silicate melts that is consistent with the available liquidus data in the haplogranite system within experimental uncertainty. The aim of such a model is the intra- and extrapolation of the experimentally determined liquidus phase equilibria for pressures up to 10 kbar and especially for H_2O-undersaturated conditions to provide a working tool applicable to most silicic magmas. Computation of phase equilibria requires an expression of the free energy of the melt as function of temperature, pressure and composition. In Section 1, we will present a parametrization of the Gibbs free energy of the melt based on the Margules approach and the computational method we used to derive an internally consistent set of solution parameters. In Section 2, model results of this study will be presented and compared with those of existing models of hydrous melts.

2. Parametrization of the Gibbs free energy of the melt

Burnham (1974) observed that the compositional dependence of H_2O fugacity in felsic melts is greatly simplified when the anhydrous composition is normalized to eight oxygens. As a consequence of this normalization, the partial molar volumes of the anhydrous mixing units assume approximately equal values and the free energy of mixing is close to ideal. In order to describe the mixing behaviour with minimum model parameters and maximum reliability, we used $NaAlSi_3O_8$, $KAlSi_3O_8$ and Si_4O_8 as endmembers of the anhydrous melt for two reasons. First, we avoid higher order excess parameters in the molar excess Gibbs free energy (G^{xs}) arising from inadequately chosen mixing components, and, second, thermodynamic properties of pure albite, orthoclase and silica melts are well constrained by experimental data at ambient *and* high pressure. H_2O was added as hypothetical oxide endmember of the hydrous melt. This approach is based on the assumption that the free energy of H_2O dissociation in silicate melts is negligible compared with changes of the bulk free energy as function of total H_2O content of the melt.

We adopted a pressure- and temperature-independent Margules-type excess polynomial to fit the remaining non-ideal mixing of the melt components in the six binary systems. Due to lack of experimental evidence, there is neither excess entropy, nor excess heat capacity, nor excess volume in the present formulation. The absence of these parameters has the advantage of a fairly stable extrapolation of G^{mix} in P and T outside the calibration range. We used three

excess parameters for the anhydrous binary melts to account for a small but complex excess heat of mixing as measured in-situ for ab–or melts by Knudsen cell mass spectroscopy (Fraser and Bottinga, 1985). We found three P,T-independent Margules parameters necessary to fit reported liquidus data in the binary systems ab–H_2O (Fenn, 1973) and qtz–H_2O (Kennedy et al., 1962), i.e. $G^{xs}=x_1x_2\cdot[W_{1112}x_1^2+W_{1122}x_1x_2+W_{1222}x_2^2]$ with the same polynomial degree, 4, as used by Clemens and Navrotsky (1987) to fit measured H^{mix} (ab–H_2O). The same excess polynomial was adapted to or–H_2O for symmetry reasons.

The ternary and quaternary excess heat of mixing was approximated from binary excess terms using a Kohler-type extrapolation method (Kohler and DeCapitani). We prefer the Kohler approach in this study because (1) the addition of numerous excess parameters is avoided in the higher order systems, (2) there is no experimental evidence suggesting additional strong ternary and quaternary interaction in order to justify additional higher order excess terms, (3) this appears promising in the perspective of an extension of the model to more complex systems (e.g. anorthite-bearing melts) and (4) in order to tightly constrain the binary excess parameters with binary, ternary, and quaternary data.

Therefore, the molar Gibbs free energy of formation (G) of the hydrous haplogranite melt is approximated with:

$$G_{\mathrm{melt}} = \sum_i x_i\left[\mu_i^0 + RT\ln(x_i)\right] + G^{xs},$$

where the summation is taken over all melt components ab, or, qtz, and H_2O; $\mu_i^0(P,T)$ being the chemical potential of pure component i:

$$\mu_i^0(P,T)=\Delta_f H_i^0 - TS_i^0 + \int C_{pi}(T)\mathrm{d}T - T\int[C_{pi}(T)/T]\mathrm{d}T + \int V_i(P,T)\mathrm{d}P$$

($\Delta_f H_i^0$ being the molar enthalpy of formation from the constituent stable elements at T_0=298.15 K and $P_0=10^5$ Pa, S_i^0 the standard molar entropy, C_{pi} the molar heat capacities, V_i molar volumes) and G^{xs} the integral molar excess heat of mixing:

$$G^{xs}=\sum x_ix_j(x_i+x_j)^{-k}[W_{iiij}x_i^2+W_{iijj}x_ix_j+W_{ijjj}x_j^2].$$

The summation is taken over all binary systems, W being the binary Margules parameters, x are mole fractions, k=2 for the Kohler extrapolation (see DeCapitani and Kirschen, 1998, for details and for computation of $RT\ln(\gamma_i)$ from G^{xs}).

The P,T-dependence of the liquid volumes was approximated by a series polynomial as used by (Berman, 1988):

$$V_{\mathrm{liq},i}(T,P)=V^0[1+v_1(T-T_0)+v_2(T-T_0)^2+v_3(P-P_0)+v_4(P-P_0)^2].$$

This approach is considered a first order approximation of $(\partial G_{\mathrm{melt}}/\partial P)_T$ for the purpose of this study because experimental ab and qtz liquidus data are reproduced, at least, to 15 kbar at dry conditions and to 5 kbar in the hydrous system. An extrapolation of the present formulation to higher pressure is difficult as complete fluid–melt miscibility is observed above 10 kbar in the SiO_2–H_2O binary system (Kennedy et al., 1962; see also Goldsmith and Shen, for ab–H_2O system). Critical mixing behaviour is, in principal, poorly modelled with two distinct equations of state for the melt and for the fluid phase. The development of a thermodynamic

model that correctly describes critical fluid–melt mixing behaviour lies outside the scope of this paper.

3. Optimization of the model parameters

Model parameters were fitted to phase equilibrium data with mathematical programming techniques. This method was introduced to thermochemical analysis by Gordon (1973) and applied to Margules-type excess parameters by Berman and Brown (1984). Advantages and disadvantages of this optimization technique and least squares refinement have been widely discussed (e.g. Berman and Powell). The strategy as applied to hydrous melts in this study is briefly described here:

Points on the liquidus surface are determined within a certain accuracy in temperature, pressure and composition by at least two experiments, thus defining a bracket on the actual equilibrium state (where the free energy of reaction LIQUID=solid, $\Delta_r G$, equals 0). Two corresponding half brackets are characterized with $\Delta_r G<0$ ("liquid stable") and $\Delta_r G>0$ ("solid stable"). For the melting of a crystalline phase, this relation is converted to:

$$\sum_i x_i \left[\mu_i^0 + RT\ln(a_i) \right] - G_s < \text{or} > 0$$

where x_i is the mole fraction, a_i the activity of melt component i, $\mu_i^0(P,T)$ from Eq. (2) and $G_s(P,T)$ is the free energy of formation of the solid. Each phase equilibrium experiment defines, at least, one constraint to G_{melt}; however, some of them are redundant. These constraints are graphically represented in Fig. 1. In the present formulation, relations (5) are linear in decision variables. Then, the optimization problem is linearly constrained and can be readily solved by large-scale linear programming methods. In evaluating a large set of linear constraints, linear programming has the advantage to yield a solution in a finite number of steps, giving a feasible solution that is consistent with all experimental half brackets. We used the software package MINOS 5.5 (Murtagh and Saunders, 1998) to prove the feasibility of the set of constraints and to solve the optimization comprising 36 variables and 496 linear constraints in the final run. $\Delta_f H^0$, S^0, $(\partial V/\partial P)_T$ of the melt endmembers, and the excess parameters W were used as fit variables. Once a feasible solution has been obtained, a selection criterion or objective function is required to define and find a unique "best" solution. We defined the objective function in order to minimize the difference between calculated and measured heats of fusion by least-squares methods.

For the crystalline phases, we applied thermochemical parameters from the updated TWQ database (Berman and Aranovich, 1996). Mixing properties of the feldspars were taken from Elkins and Grove (1990). H_2O and SiO_2 solution in the feldspars was neglected and we assumed pure silica polymorphs. To further constrain μ_i^0 of melt components, we used reported C_p and ΔH_{fus} data from Richet and Bottinga (1986) and C_{pH2O} from Richet (1987) as first estimate. Liquid volume parameters V^0 and v_1 were taken from Knoche et al. (1995), v_3 and v_4 were fitted to experimental data.

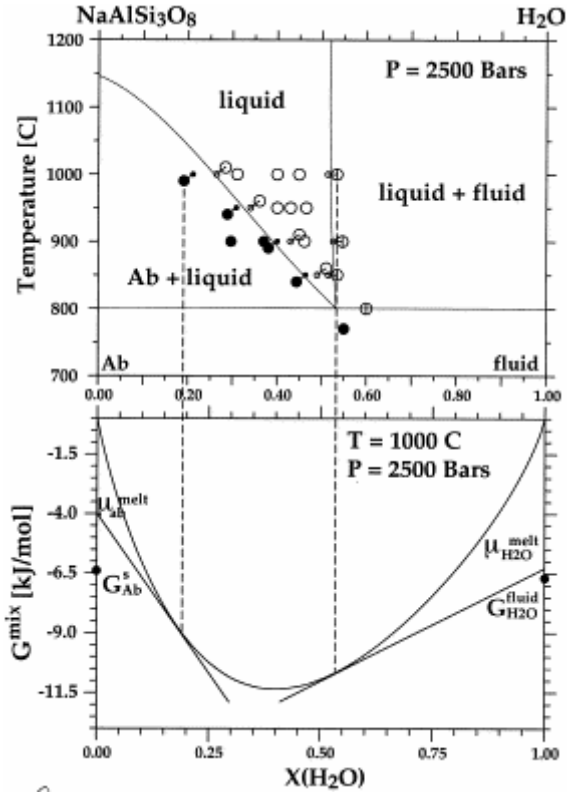


Fig. 1. Assessment of quench experiments in the system $NaAlSi_3O_8$–H_2O. Symbols point to quench of albite+liquid (•), one liquid (○) and liquid+fluid phase (slashed open circles) from Fenn (1973). Calculated stability field boundaries are from this study. Constraints are relaxed to account for experimental uncertainty (±10°C and 2 mol% H_2O). Each experiment yields at least one inequality constraint to the free energy of the hydrous melt with respect to the free energy of albite or fluid.

Solution parameters were fitted to phase equilibrium data in the endmember systems $NaAlSi_3O_8$ (Boettcher et al., 1982), $KAlSi_3O_8$ (Lindsley and Boettcher), SiO_2 (Hudon, 1998), and in the hydrous systems, $NaAlSi_3O_8$–$KAlSi_3O_8$–H_2O (Fenn, 1973), and $NaAlSi_3O_8$–$KAlSi_3O_8$–SiO_2–H_2O (Steiner, 1970; Holtz; Pichavant and Becker). We preferred these data in the optimization of the hydrous melt parameters because (1) experiments were performed at both H_2O-saturated and -undersaturated conditions and (2) the H_2O content of the melt is reasonably well known (determined either from the H_2O content of the bulk charge or from the KFT analysis of the quenched glasses). Additional constraints below 6 kbar stem from H_2O-saturated melting experiments in the systems SiO_2–H_2O (Kennedy et al., 1962), $NaAlSi_3O_8$–H_2O (Goldsmith and Jenkins, 1985), and $KAlSi_3O_8$–H_2O (Goldsmith and Peterson, 1990). Water contents of the quenched glasses were taken from Holtz; Holtz and Holtz, Behrens (1995), and Behrens at al. (2000). Solubilities at 1100°C from Kennedy et al. (1962) determined with the weight loss method were substituted by KFT data from Holtz et al. (2000). Variation of H_2O solubility was assumed to be less than ±0.2 wt.% when extrapolated from 1200°C to 1100°C below 4 kbar. All halfbrackets were relaxed by considering conservative overall experimental uncertainties in temperature (±15°C for experiments at 1000°C from Steiner (1970), ±10°C else) and composition (±2 mol%).

As H_2O solubility in the crystalline phases is neglected, ΔH_{fus} measurements and liquidus data constrain the chemical potentials of ab, or, and qtz in the melt (i.e. H^0, S^0, v_3, and v_4, and W), but not the chemical potential of the H_2O melt component, $\mu_{H2O}=\mu_{H2O}{}^0+RT\ln(a_{H2O})$. In order to estimate the chemical potential of pure H_2O melt ($\mu_{H2O}{}^0$), we used H_2O solubility data as

additional constraints below 3 kbar and 1200°C (see Fig. 1). The merit of these constraints on μ_{H2O}^{0} increases as the H_2O activity in the melt is fixed by liquidus constraints through the Gibbs–Duhem relation. Due to the large experimental database in the haplogranite system and the fairly stable excess function, this approach is therefore justified. The free energy of the supercritical fluid, G_s in Eq. (5), was approximated with the Haar et al. (1984) equation of state. Neglect of melt dissolution in the fluid (e.g. 2.4 mol% qtz at 1080°C, 3.0 kbar, Kennedy et al., 1962) leads to an estimated error to μ_{H2O}^{fluid} of the order $RT \ln(x_{H2O})=-270$ J/mol. To avoid an erroneous reduction of the extent of the feasible region from an overestimated G_{fluid}, we skipped "fluid stable" constraints above 2.5 kbar and 1100°C. Therefore, the H_2O saturation surface is overestimated at $P>3$ kbar and $T>1100$°C when calculated with a pure H_2O fluid phase. In a subsequent step, we have to substitute the Haar et al. (1984) equation of state of pure H_2O with a multicomponent solution model that incorporates dissolution of ab, or, and qtz melt components in the fluid. Such a solution model is not available at the moment. For this purpose, accurately determined fluid–melt compositions are required in addition to crystalline–fluid phase equilibrium data at elevated temperatures, e.g. Bai and Koster van Groos (1999). Direct volume measurements of ab–H_2O melts from Burnham and Davis (1971) were not incorporated in the present study, because they used Ca-bearing natural starting material. Due to these limitations, we do not refine additional volume terms as $V_{liq}(T,P)=\sum_{i,j} a_{ij} P^i T^j$ (Burnham and Davis, 1971) from H_2O solubility data. Such refinements will significantly improve the reliability of the predicted solubility surface at supraliquidus temperature and $P>5$ kbar but it is of minor importance for liquidus phase relations of the present study.

Thermochemical parameters of crystalline and liquid oxides used in this study are given in Table 1, Table 2 and Table 3. Margules-type excess parameters are listed in Table 4. Inconsistencies between calculated and observed phase relations remain for experiments no. 413 (Kfs out), from Steiner (1970) and experiment [5 kbar, 820°C, $x_{H2O}=0.7$, glass no. $2_5 34_5$, Fsp in] from Holtz et al. (1992b). This may be a consequence of the deviation from the ab–or–qtz composition plane (1) by Na contamination that affected the starting gels used by Luth et al. (1964) and Steiner (1970) as discussed in Holtz et al. (1992b) and (2) due to 1.7 normative corundum of the quenched glass (Holtz et al., 1992b).

Table 1. Standard state thermochemical properties of solid and liquid oxides

H_2O fluid, see text. $T_0=298.15$ K, $P_0=1$ bar.

	Abbreviation	Formula	$\Delta_f H^0$ [J/mol]	S^0 [J/K mol]	Reference
α-Cristobalite	α-Crist	SiO_2	−907 753.35	43.3943	Berman (1988)
β-Cristobalite	β-Crist	SiO_2	−906 377.23	46.0288	Berman (1988)
α-Quartz	α-Qz	SiO_2	−910 699.95	41.4600	Berman (1988)
β-Quartz	β-Qz	SiO_2	−908 626.77	44.2068	Berman (1988)
low-Tridymite	l-Trid	SiO_2	−907 749.56	43.7702	Berman (1988)
high-Tridymite	h-Trid	SiO_2	−907 045.12	45.5237	Berman (1988)
Albite	Ab	$NaAlSi_3O_8$	−3 921 618.20	224.4120	Berman (1988)
K-feldspar	Kfs	$KAlSi_3O_8$	−3 970 790.78	214.1451	Berman (1988)
Ab liq	ab	$NaAlSi_3O_8$	−3 903 511.00	191.4476	this study
Or liq	or	$KAlSi_3O_8$	−3 935 320.00	217.0192	this study
Qtz liq	qtz	Si_4O_8	−3 679 484.00	71.6667	this study
H_2O liq	H_2O	H_2O	−286 748.50	67.1751	this study

Table 2. Volume parameters used in this study

$V(T,P)=V_0[1+v_1(T-T_0)+v_2(T-T_0)^2+v_3(P-P_0)+v_4(P-P_0)^2]$ in J/bar, T in K, P in bar, T_0=298 K, P_0=1 bar.

	V_0 [J/bar]	v_1 [10^5/K]	v_2 [10^5/K^2]	v_3 [10^5/bar]	v_4 [10^8/bar^2]	Reference
α-Cristobalite	2.587	2.08240619	0	−0.25145068	0	Berman (1988)
β-Cristobalite	2.730	0.31892080	0	−0.10997269	0	Berman (1988)
α-Quartz	2.269	2.38945698	0	−0.24339298	0.00101375	Berman (1988)
β-Quartz	2.370	0	0	−0.12382672	0.00070871	Berman (1988)
low-Tridymite	2.675	1.93394983	0	−0.25084238	0	Berman (1988)
high-Tridymite	2.737	0.48286524	0	−0.07396833	0.00037354	Berman (1988)
Albite	10.083	2.63072032	0.00032407	−0.19446932	0.00048611	Berman (1988)
K-feldspar	10.869	1.51450750	0.00054850	−0.18045110	0.00051120	Berman (1988)
Ab liq	9.437	23.04500000	0	−2.92533477	0.11517438	this study[a]
Or liq	10.112	21.51100000	0	−2.39792453	0.06287995	this study[a]
Qtz liq	10.691	2.81800000	0	−1.60660444	0.05337397	this study[a]
H_2O liq	1.200	56.83363333	0.03676951	−0.03441358	1.06892250	this study[b]

Table 3. C_p coefficients used in this study

	k_1	k_2	k_4	k_3	k_8	Reference
α-Cristobalite	83.5136	0	−374.693	−2 455 360	280 072 192	Berman and Brown (1985)[a]
β-Cristobalite	83.5136	0	−374.693	−2 455 360	280 072 192	Berman and Brown (1985)
α-Quartz	80.01199	0	−240.276	−3 546 684	491 568 384	Berman and Brown (1985)[b]
β-Quartz	80.01199	0	−240.276	−3 546 684	491 568 384	Berman and Brown (1985)
low-Tridymite	75.3727	0	0	−5 958 095	958 246 144	Berman (1988)[c]
high-Tridymite	75.3727	0	0	−5 958 095	958 246 144	Berman (1988)
Albite	393.6357	0	−2415.498	−7 892 826	1070 636 032	Berman (1988)[d]
K-feldspar	381.3723	0	−1941.045	−12 037 252	1836 425 472	Berman and Brown (1985)[e]
Ab liq	300.6700	0.042620	0	0	0	Richet and Bottinga (1984)
Or liq	261.8400	0.061872	0	0	0	Richet and Bottinga (1984)
Qtz liq	325.4920	0	0	0	0	Richet and Bottinga (1984)
H_2O liq	81.4370	0.000098	0	−3 109 400	0	Richet (1987)

C_p function used in this study: $C_p = k_1 + k_2T + k_3/T^2 + k_4/\sqrt{T} + k_8/T^3$ in J/K mol.

[a] λ transition modelled with additional $C_p = (T - dT)[-0.14216187 + 0.0044142(T - dT)]^2$ between $[298K + dT,\ 535K + dT]$, $dT = 0.048\ (P - P_0)$ (Berman and Brown, 1986).

[b] λ transition modelled with additional $C_p = (T - dT)[-0.09186959 + 0.00024607(T - dT)]^2$ between $[373K + dT,\ 848K + dT]$, $dT = 0.023743(P - P_0)$ (Berman and Brown, 1986).

[c] λ transition modelled with additional $C_p = (0.42670490 - 0.00144575)^2$ between $[298K,\ 390K]$ (Berman, 1988).

[d] C2/m-C $\bar{1}$ transition modelled with Landau-type ordering parameters, (Salje, 1985).

[e] T-dependent disordering approximated with additional $C_p = 282.98291 - 4831.375/\sqrt{T} + 3620706./T^2 - 0.15733T + 0.00003T^2$ between $[298K,\ 1436K]$, (Berman, 1988).

4. Model results and discussion

Reported high pressure fusion data of pure SiO_2 from Jackson (1976) are not consistent with all other β-Qz melting data in the hydrous systems. Calculated melting temperatures of pure silica are 30°C to 50°C higher when projected to perfectly dry conditions. This suggests that Jackson's starting material had been contaminated before or during the run in a pyrophyllite-bearing high-pressure assembly. Therefore, we used SiO_2 fusion data from Hudon (1998) that were obtained using an anhydrous piston-cylinder apparatus (Hudon et al., 1994). Calculated fusion curves of pure $NaAlSi_3O_8$, $KAlSi_3O_8$ and SiO_2 are shown in Fig. 2.

Table 4. Margules-type excess parameters used in this study

Ab-Kfs Feldspar, Elkins and Grove (1990)[a]	W_H	W_S	W_V
112	18810	10.30	0.4602
122	27320	10.30	0.3264

Melt, this study[b]	W_{1112}	W_{1122}	W_{1222}	k
ab–qtz	25503.980	−17245.030	8673.084	2
or–qtz	8622.563	−5946.898	−7150.107	2
ab–or	13969.360	−30153.510	6921.565	2
ab–H_2O	−32471.070	−21823.540	−2926.132	2
or–H_2O	−24849.790	−14857.800	1723.691	2
qtz–H_2O	−27423.890	6269.606	9927.726	−3

[a] $G^{xs}(T,P) = x_1 x_2[W_{112} x_1 + W_{122} x_2]$, $W = W_H - TW_S + (P - P_0)W_V$, W in J/mol, T in K, P in bars, $P_0 = 1$ bar.

[b] $G^{xs} = \Sigma x_1 x_2 (x_1 + x_2)^{-k}[W_{1112} x_1^2 + W_{1122} x_1 x_2 + W_{1222} x_2^2]$, W in J/mol.

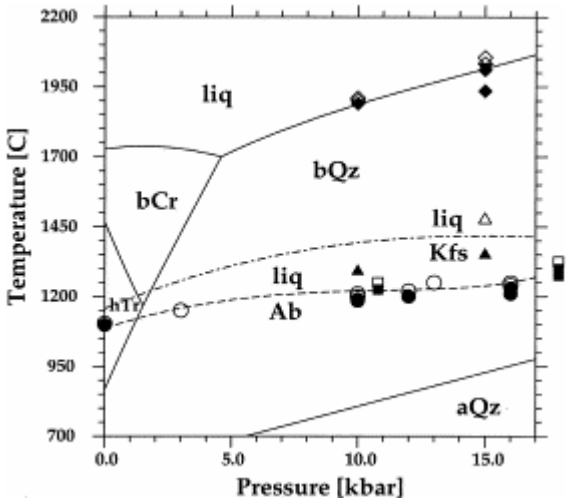


Fig. 2. Calculated fusion curves of $NaAlSi_3O_8$, $KAlSi_3O_8$, Si_4O_8. Calculated stability field boundaries of anhydrous $NaAlSi_3O_8$ (dashed line), $KAlSi_3O_8$ (dash-dotted line), Si_4O_8 (solid line) using Eq. (4) compared with experimental data. Open symbols denote liquid stable, solid symbols point crystalline phase stable; diamonds are from Hudon (1998), triangles from Lindsley (1966), circles from Boettcher et al. (1982), squares from Boyd and England (1963, not used in the optimization). Calculated Kfs melting is metastable with respect to incongruent melting to a liquid and leucite.

Fitted heats of fusion (67.4 kJ/mol $NaAlSi_3O_8$, 58.0 kJ/mol $KAlSi_3O_8$, 35.6 kJ/mol Si_4O_8) are close to reported values from Richet and Bottinga (1986) (64.3±3, 54.0±4, 35.7±1 kJ/mol, respectively). The fitted heat of mixing surface of the anhydrous melt is plotted in Fig. 3. Calculated G^{xs} of ab–or and qtz–or liquid is close to zero; ab–qtz mixing shows a small positive deviation from an ideal solution. This is in rough agreement with solution calorimetry measurements of ab–or–qtz glasses indicating slightly positive heats of mixing for ab–qtz (Navrotsky et al., 1980), small positive and negative heats of mixing for or–qtz, and negative heats of mixing for ab–or (Hervig and Navrotsky, 1984). Fraser and Bottinga (1985) reported positive heats of mixing at or-rich composition from in-situ measurements at 1200–1600°C. This indicates a small temperature dependency of H^{mix} in ab–or liquids, which is probably

averaged by the T-independent H^{mix} model in this study. However, the precision of the fitted enthalpies of the liquid feldspar endmembers is not better than 3 kJ due to the uncertainty of heat of fusion measurements and thermochemical data of the crystalline reference phases (see, e.g. Arnorsson and Stefansson, 1999, for a review and discussion).

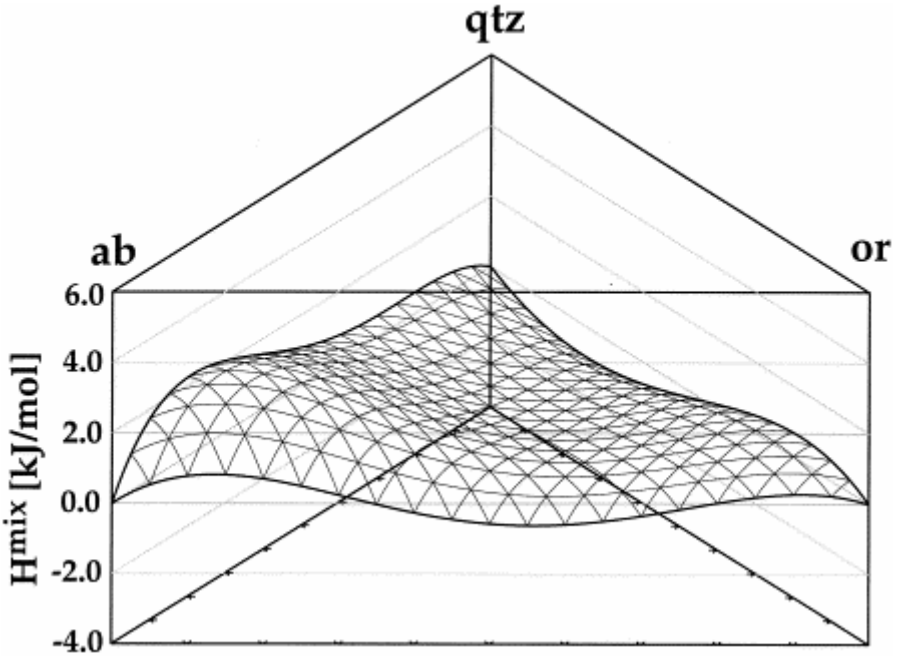


Fig. 3. Fitted G^{xs} surface of the anhydrous melt. Calculated P,T-independent H^{mix} surface of the anhydrous melt components shows small but complex departure from ideality.

Calculated isotherms of the liquidus surface in the system $NaAlSi_3O_8$–$KAlSi_3O_8$–H_2O are shown in Fig. 4. Calculated phase relations at 2 and 5 kbars in the systems $NaAlSi_3O_8$–Si_4O_8–H_2O and $KAlSi_3O_8$–Si_4O_8–H_2O are plotted in Fig. 5 and Fig. 6. Predicted crystal–liquid equilibria are in close agreement with experimental data at H_2O-saturated and -undersaturated conditions. However, the calculated liquid–fluid coexistence curve overestimates H_2O solubility with increasing temperature due to neglect of melt dissolution.

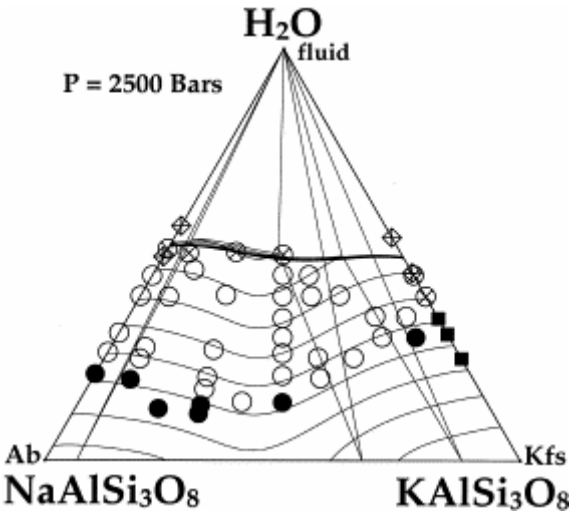


Fig. 4. Calculated isotherms on the liquidus surface in the system $NaAlSi_3O_8$–$KAlSi_3O_8$–H_2O at 2500 bars, 800°C to 1200°C with 50°C increments, from this study compared with results from quench experiments at 1000±10°C (Fenn, 1973). Solid circles are quench of liquid+feldspar, open symbols point one liquid, slashed

circles are liquid+fluid. Slashed diamonds are solubility data from Behrens et al. (2000) at 2 and 3 kbars, 1000°C (ab) and 1200°C (or), respectively. Leucite stability field (solid squares) is omitted.

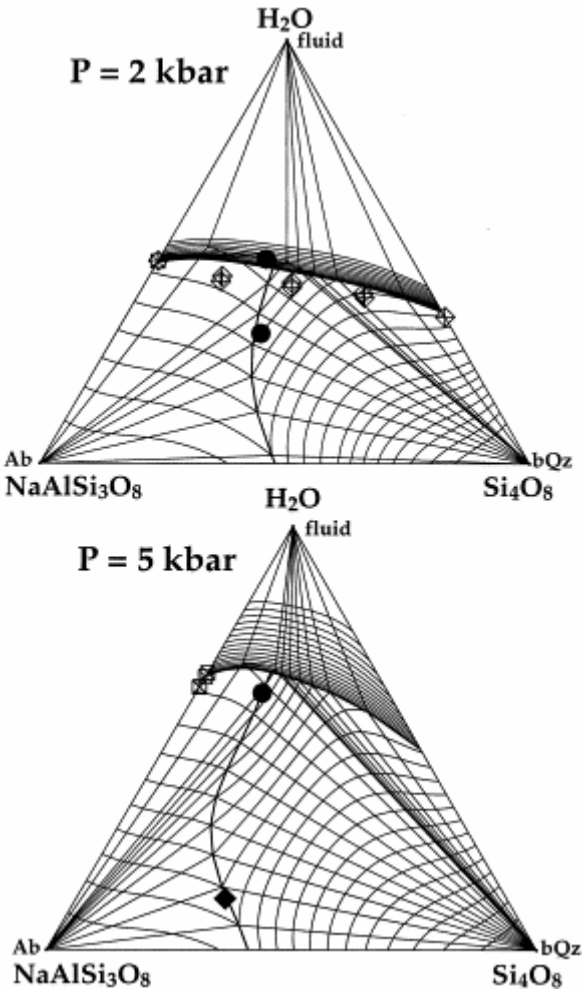


Fig. 5. Calculated isotherms on the liquidus surface in the system $NaAlSi_3O_8$–Si_4O_8–H_2O at 2 and 5 kbars, 700°C to 1700°C with 50°C increments. Solid symbols denote measured compositions of minimum melting at H_2O-saturated and -undersaturated conditions from Pichavant et al. (1992); 680°C, 740°C, 860°C, circles and Becker et al. (1998); 1095±10°C, diamond. Open diamonds are measured H_2O solubility at 1200°C and 1300°C (Holtz et al., 2000). Squares are solubility data at 825°C, 2 kbars and 860°C to 1200°C, 5 kbars from Behrens et al. (2000).

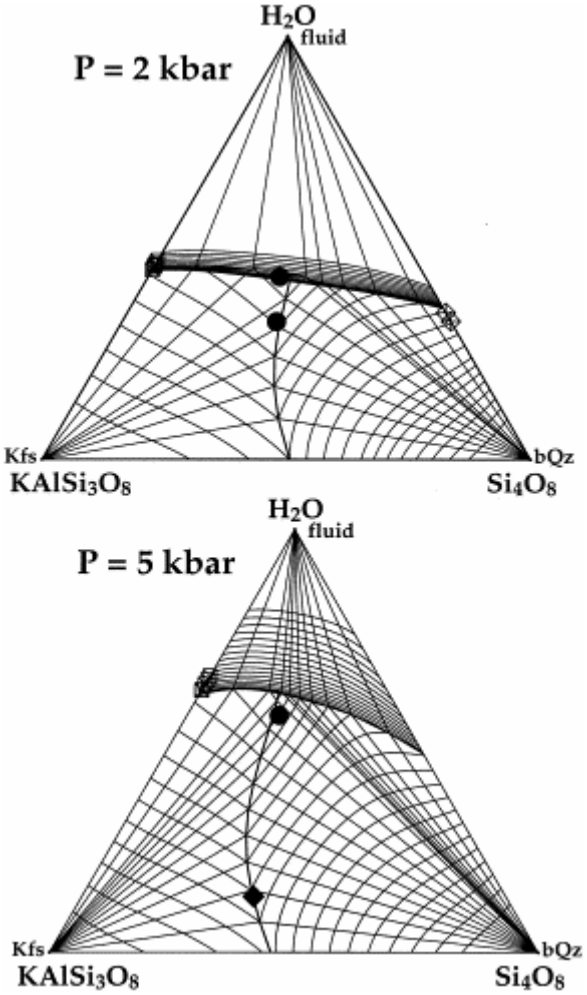


Fig. 6. Calculated isotherms on the liquidus surface in the system $KAlSi_3O_8$–Si_4O_8–H_2O at 2 and 5 kbars, 700°C to 1700°C with 50°C increments. Solid symbols denote measured compositions of minimum melting at H_2O-saturated and -undersaturated conditions from Pichavant et al. (1992); 720°C, 750°C, 835°C, circles and Becker et al. (1998); 1030±10°C, diamond. Open diamonds are measured H_2O solubility at 1200°C and 1300°C (Holtz et al., 2000). Squares are solubility data at 1000°C, 2 kbars and 900°C to 1200°C, 5 kbars from Behrens et al. (2000).

Exothermic heats of mixing were fitted in the ab–H_2O and or–H_2O systems at water-undersaturated compositions; qtz–H_2O mixing is more complex containing a considerable positive excess term. This is consistent with observations in earlier studies, e.g. Shaw (1964), Clemens and Navrotsky (1987), Blencoe (1992) and Ghiorso and Sack (1995). The positive excess heat of mixing leads to a considerable metastable miscibility gap of the SiO_2–H_2O liquid at high H_2O composition. We found a T-independent excess function adequate to describe experimental data within experimental uncertainty in the system ab–H_2O at 2.5 kbar (Fenn, 1973) (see Fig. 1). Fitted absolute ab–H_2O excess heat of mixing is less than measured by Clemens and Navrotsky (1987). The calculated minimum at x_{H2O}=0.32 is in reasonable agreement with their estimate (0.27). The remaining discrepancy can be reduced by assuming a T-dependent G^{xs} as suggested by Blencoe (1992), e.g. $W=W_H-TW_S+[T-T_0-T\ln(T/T_0)]W_{Cp}$. However, small positive excess entropy (W_S) or negative excess heat capacity (W_{Cp}) parameters were not included in the present formulation of H^{mix}, because they are not needed to fit experimental liquidus phase equilibrium data to 1100°C. A small negative C_p^{xs} indicates

that $C_{pH2O,liq}$ is slightly underestimated with $C_{pH2O,glass}$ (Richet, 1987) when extrapolated beyond the glass transition.

Using a Kohler extrapolation for the Si_4O_8–H_2O excess function (k=2) the calculated stability field of β-Qz was strongly inconsistent with experiments from Holtz et al. (1992b), Pichavant et al. (1992), and Becker et al. (1998). A positive Si_4O_8–H_2O excess function at x_{H2O}>0.58 increases the free energy of mixing of the melt when extrapolated to the higher order system and, thus, leads to a larger calculated β-Qz stability field than measured at water-undersaturated compositions. In order to reduce the extrapolated qtz–H_2O contribution to G^{mix} of the melt k was set to −3 giving, indeed, a feasible region of the experimental qtz constraints. The use of k=−3 increases the polynomial degree of G^{xs}(qtz–H_2O) from four to seven only for extrapolation purposes and leads to a strong decrease of the binary excess contribution in the higher order system, where $x_{qtz}+x_{H2O}<1$. This suggests that (1) two distinct mixing mechanisms are attributed to feldspar–H_2O and silica–H_2O melts and (2) the latter contributes to a very minor degree to the haplogranite system.

Experimentally determined liquidus phase relations from Holtz et al. (1992b) are in good agreement with predictions of the model of Burnham and Nekvasil (1986), revised in Nekvasil and Burnham (1987), for H_2O-saturated isobaric sections. However, the calculated β-Qz liquidus primary field increases with decreasing $a(H_2O)$ shifting the minimum liquidus composition towards the ab–or join in contrast to experimental data (Holtz et al., 1992b). At H_2O-undersaturated conditions H_2O–qtz mixing is approximated as an ideal Henryan solution: a_{qtz}□$(1-x_{H2O})^2$ for $x_{H2O}<0.5$ (Burnham and Nekvasil, 1986; their Eq. 5). This relation is independent of the anhydrous composition, even if non-ideal mixing of the anhydrous components is considered with a separate term (Nekvasil and Burnham, 1987). We believe, that this formulation overestimates a_{qtz} when extrapolated to the haplogranite system in discrepancy with experiments. In this study, we used a polynomial of degree 7 for G^{xs} (qtz–H_2O); its contribution to a_{qtz} decreases drastically in the multicomponent system.

MELTS incorporates a similar parametrization of the effect of water on magmatic phase equilibria (Ghiorso and Sack, 1995). Ghiorso and Sack (1995) included H_2O as oxide component of the melt, with $\Delta_f H^0$=−280 kJ/mol, S^0=152.6 J/K mol and a corrected $V(T,P)$ polynomial from Nicholls (1980) and refined regular solution parameters of the melt, i.e. $G^{xs}=1/2\sum_{i,j}W_{ij}x_ix_j$, using "anhydrous" and H_2O-saturated experimental liquidus data at magmatic compositions. We are aware that the merit of MELTS is the application to magmatic liquids. The projection of the thermodynamic model of the melt to bounding compositional subsystems outside the calibration range is not warranted as stated by Ghiorso and Sack (1995). Bearing this restriction in mind, the calculated liquidus temperatures and Fsp compositions using the public version MELTS-HP 2.0.4 yield an acceptable first-order approximation (within 10–60°C and 5 mol%) in the haplogranite system when compared to the experimental results at very low H_2O activities from Becker et al. (1998). However, in all cases the calculated SiO_2-saturation surface is at higher SiO_2 content and lower temperature than observed and, regarding the experiments from Pichavant et al. (1992) and Holtz et al. (1992b), the difference between calculated and observed liquidus temperatures increases systematically (to 110°C) with increasing H_2O content and decreasing temperature. This indicates that an overestimated absolute $\mu_{H2O}{}^0$ is compensated with the H_2O melt excess parameters W_{ij} when fitted to multicomponent data in H_2O-saturated systems. However, direct comparison of the fitted free energy of mixing surface is difficult due to the different choice of anhydrous melt endmember compositions.

5. Conclusions

(1) We expanded the Margules approach as applied to $NaAlSi_3O_8$–H_2O by Blencoe (1992) to hydrous haplogranite melts. Applying mathematical programming techniques, internally consistent thermochemical data for the hydrous melt have been derived from experimental phase equilibrium data. Using both experimental liquidus and solubility data and a simple approximation of the liquid molar volume, standard state thermochemical properties of the hypothetical H_2O melt oxide component were estimated close to $\Delta_f H^0$=−287 kJ/mol and S^0=67.2 J/K mol, respectively. Fitted $(\partial V/\partial T)_P$ and $(\partial V/\partial P)_T$ parameters indicate extremely high thermal expansivity and compressibility of the H_2O melt component as observed by Ochs and Lange (1997).

(2) Assuming $NaAlSi_3O_8$, $KAlSi_3O_8$ and Si_4O_8 as anhydrous melt components and using measured heats of fusion from Richet and Bottinga (1986), we found a small, but complex excess heat of mixing necessary to reproduce reported liquidus phase equilibria.

(3) Thermodynamic assessment of phase equilibrium data from Holtz et al. (1992b), Pichavant et al. (1992) and Becker et al. (1998) suggests that two mixing mechanisms can be attributed to feldspar–H_2O and qtz–H_2O melts. Enthalpies of mixing of feldspar–H_2O are negative to $x(H_2O)$=0.9 (or) and 1.0 (ab), while qtz–H_2O mixing displays positive excess contributions at $x(H_2O)$>0.58. The latter contributes to a very minor degree to the haplogranite system.

Acknowledgements

C. DeCapitani wrote the initial version of the optimization routine. We thank H. Nekvasil for generously providing us with her EQUIL90 source code. H. Behrens, F. Holtz and P. Hudon communicated experimental data prior to publication. Helpful comments from P. Asimov and C. Romano on an earlier draft of the manuscript are appreciated. This work was financially supported by the EC-TMR network “In-situ Hydrous Melts” (contract no. ERBFMRXCT960063).

References

Bai, T.B. and Koster van Groos, A.F., 1999. The distribution of Na, K, Rb, Sr, Al, Ge, Cu, W, Mo, La, and Ce between granitic melts and coexisting aqueous fluids. *Geochim. Cosmochim. Acta* **63**, pp. 1117–1131.

Becker, A., Holtz, F. and Johannes, W., 1998. Liquidus temperatures and phase compositions in the system Qz–Ab–Or at 5 kbar and very low water activities. *Contrib. Mineral. Petrol.* **130**, pp. 213–224.

Behrens, H., 1995. Determination of water solubilities in high-viscosity melts: an experimental study on $NaAlSi_3O_8$ and $KAlSi_3O_8$ melts. *Eur. J. Mineral.* **7**, pp. 905–920.

Behrens, H., Romano, C., Nowak, M., Holtz, F. and Dingwell, D.B., 1996. Near-infrared spectroscopic determination of water species of the system $MAlSi_3O_8$ (M=Li, Na, K): an interlaboratory study. *Chem. Geol.* **128**, pp. 41–63.

Behrens, H., Meyer, M., Benne, D., Nowak, M. and Holtz, F., 2000. Temperature and pressure dependence of water solubility in melts of $MAlSi_3O_8$ (M=Li, Na, K, Rb) endmember compositions. *Chem. Geol.* submitted.

Berman, R.G., 1988. Internally consistent thermodynamic data for minerals in the system Na_2O–K_2O–CaO–MgO–FeO–Fe_2O_3–Al_2O_3–SiO_2–TiO_2–H_2O–CO_2. *J. Petrol.* **29**, pp. 445–522.

Berman, R.G. and Brown, T.H., 1984. A thermodynamic model for multicomponent melts with application to the system CaO–$Al2O_3$–SiO_2. *Geochim. Cosmochim. Acta* **48**, pp. 661–678.

Berman, R.G. and Brown, T.H., 1985. Heat capacities of minerals in the system Na_2O–K_2O–CaO–MgO–FeO–Fe_2O_3–Al_2O_3–SiO_2–TiO_2–H_2O–CO_2: representation, estimation, and high temperature extrapolation. *Contrib. Mineral. Petrol.* **89**, pp. 168–183.

Berman, R.G. and Brown, T.H., 1986. Erratum: heat capacities of minerals in the system Na_2O–K_2O–CaO–MgO–FeO–Fe_2O_3–Al_2O_3–SiO_2–TiO_2–H_2O–CO_2: representation, estimation, and high temperature extrapolation. *Contrib. Mineral. Petrol.* **94**, p. 262.

Berman, R.G., Engi, M., Greenwood, H.J. and Brown, T.H., 1986. Derivation of internally consistent thermodynamic data by the technique of mathematical programming: a review with application to the system MgO–SiO_2–H_2O. *J. Petrol.* **27**, pp. 1331–1364.

Berman, R.G. and Aranovich, L.Y., 1996. Optimized standard state and solution properties of minerals: I. Model calibration for olivine, orthopyroxene, cordierite, and ilmenite in the system FeO–MgO–CaO–H_2O. *Contrib. Mineral. Petrol.* **126**, pp. 1–24.

Blencoe, J.G., 1992. A two-parameter Margules method for modelling the thermodynamic mixing properties of albite–water melts. *Trans. R. Soc. Edingburgh: Earth Sci.* **83**, pp. 423–428.

Boettcher, A., Burnham, C., Windom, K. and Bohlen, S., 1982. Liquids, glasses, and the melting of silicates to high pressures. *J. Geol.* **90**, pp. 127–138.

Boettcher, A., Guo, Q., Bohlen, S. and Hanson, B., 1984. Melting in feldspar-bearing systems to high pressures and structures of aluminosilicate liquids. *Geology* **12**, pp. 202–204.

Boyd, F.R. and England, J.L., 1963. Effect of pressure on the melting of diopside $CaMgSi_2O_8$ and albite $NaAlSi_3O_8$ in the range up to 50 kilobars. *J. Geophys. Res.* **68**, pp. 311–323.

Bowen, N.L. and Tuttle, O.F., 1950. The system $NaAlSi_3O_8$–$KAlSi_3O_8$–H_2O. *J. Geol.* **58**, pp. 489–511.

Burnham, C.W., 1974. $NaAlSi_3O_8$–H_2O solutions: a thermodynamic model for hydrous silicate magmas. *Bull. Soc. Fr. Mineral. Cristallogr.* **97**, pp. 223–230.

Burnham, C.W. and Davis, N.F., 1971. The role of H_2O in silicate melts: I. *P–V–T* relations in the system $NaAlSi_3O_8$–H_2O to 10 kilobars and 1000°C. *Am. J. Sci.* **270**, pp. 54–79.

Burnham, C.W. and Nekvasil, H., 1986. Equilibrium properties of granite pegmatite magmas. *Am. Mineral.* **71**, pp. 239–263.

Clemens, J.D. and Navrotsky, A., 1987. Mixing properties of $NaAlSi_3O_8$ melt–H_2O: new calorimetric data and some geological implications. *Geochim. Cosmochim. Acta* **95**, pp. 173–186.

DeCapitani, C. and Kirschen, M., 1998. A generalized multicomponent excess function with application to immiscible liquids in the system CaO–SiO_2–TiO_2. *Geochim. Cosmochim. Acta* **62**, pp. 3753–3763.

Elkins, L.T. and Grove, T.L., 1990. Ternary feldspar experiments and thermodynamic models. *Am. Mineral.* **75**, pp. 544–559.

Fenn, P.M., 1973. Nucleation and growth of alkali feldspars from melts in the system $NaAlSi_3O_8$–$KAlSi_3O_8$–H_2O. PhD dissertation, Stanford University, 167 pp.

Fraser, D.G. and Bottinga, Y., 1985. The mixing properties of melts and glasses in the system $NaAlSi_3O_8$–$KAlSi_3O_8$: comparison of experimental data obtained by Knudsen mass spectroscopy and solution calorimetry. *Geochim. Cosmochim. Acta* **49**, pp. 1377–1381.

Ghiorso, M.S. and Sack, R.O., 1995. Chemical mass transfer in magmatic processes: IV. A revised and internally consistent thermodynamic model for the interpolation and extrapolation of liquid–solid equilibria in magmatic systems at elevated temperatures and pressures. *Contrib. Mineral. Petrol.* **119**, pp. 197–212.

Goldsmith, J.R. and Jenkins, D.M., 1985. The hydrothermal melting of low and high albite. *Am. Mineral.* **70**, pp. 924–933.

Goldsmith, J.R. and Peterson, J.W., 1990. The hydrothermal melting behaviour of $KAlSi_3O_8$ as microcline and sanidine. *Am. Mineral.* **75**, pp. 1362–1469.

Goranson, R.W., 1931. The solubility of water in granite magmas. *Am. J. Sci.* **22**, pp. 481–502.

Goranson, R.W., 1932. Some notes on the melting of granite. *Am. J. Sci.* **23**, pp. 227–236.

Gordon, T.M., 1973. Determination of internally consistent thermodynamic data from phase equilibrium experiments. *J. Geol.* **81**, pp. 199–208.

Haar, L., Gallagher, J.S. and Kell, G.S., 1984. *NBS/NRC Steam Tables: Thermodynamic and Transport Properties and Computer Programs for Vapor and Liquid States of Water in SI Units*, Hemisphere Publishing.

Hervig, R.L. and Navrotsky, A., 1984. Thermochemical study of glasses in the system $NaAlSi_3O_8$–$KAlSi_3O_8$–Si_4O_8 and the join $Na_{1.6}Al_{1.6}Si_{2.4}O_8$–$K_{1.6}Al_{1.6}Si_{2.4}O_8$. *Geochim. Cosmochim. Acta* **48**, pp. 513–522.

Holtz, F., Behrens, H., Dingwell, D. and Johannes, W., 1995. H_2O solubility in haplogranitic melts: compositional, pressure, and temperature dependence. *Am. Mineral.* **80**, pp. 94–108.

Holtz, F., Behrens, H., Dingwell, D. and Taylor, R.P., 1992. Water solubility in aluminosilicate melts of haplogranite composition at 2 kbar. *Chem. Geol.* **96**, pp. 289–302. Abstract

Holtz, F., Pichavant, M., Barbey, P. and Johannes, W., 1992. Effects of H_2O on liquidus phase relations in the haplogranite system at 2 and 5 kbar. *Am. Mineral.* **77**, pp. 1223–1241.

Holtz, F., Roux, J., Behrens, H. and Pichavant, M., 2000. Water solubility in silica and quartzofeldspathoic aluminosilicate melts. *Eur. J. Mineral.* **85**, pp. 682–686.

Hudon, P., 1998. The study of melts in the ternary CaO–MgO–SiO_2 at high pressure and the nature of immiscibility in binary systems. PhD Thesis, McGill University, Montreal, 362 pp.

Hudon, P., Baker, D. and Toft, P.B., 1994. A high-temperature assembly for 1.91-cm (3/4″) piston-cylinder apparatus. *Am Mineral.* **79**, pp. 145–147.

Jackson, I., 1976. Melting of silica isotypes SiO_2, BeF_2 and GeO_2 at elevated pressures. *Phys. Earth Planet. Inter.* **13**, pp. 218–231.

Kennedy, G.C., Wasserburg, G.J., Heard, H.C. and Newton, R.C., 1962. The upper three-phase region in the system SiO_2–H_2O. *Am. J. Sci.* **260**, pp. 501–521.

Knoche, R., Dingwell, D.B. and Webb, S.L., 1995. Melt densities for leucogranites and granitic pegmatites: partial molar volumes for Al_2O_3, Na_2O, K_2O, Li_2O, Rb_2O, Cs_2O, MgO, CaO, SrO, BaO, B_2O_3, P_2O_5, F_2O_{-1}, TiO_2, Nb_2O_5, Ta_2O_5, and WO_3. *Geochim. Cosmochim. Acta* **59**, pp. 4645–4652.

Kohler, F., 1960. Zur Berechnung der thermodynamischen Daten eines ternaeren Systems aus den zugehoerigen binaeren Systemen. *Monatsh. Chem.* **91**, pp. 738–740.

Lindsley, D.H., 1966. Melting relations of $KAlSi_3O_8$: effect of pressures up to 40 kilobars. *Am. Mineral.* **51**, pp. 1793–1799.

Luth, W.C., Jahns, R.H. and Tuttle, O.F., 1964. The granite system at pressures of 4 to 10 kilobars. *J. Geophys. Res.* **69**, pp. 759–773.

Murtagh, B.A., Saunders, M.A., 1998. MINOS 5.5. User's Guide (technical report SOL 83-20R, revised). Systems Optimization Laboratory, Stanford University.

Navrotsky, A., Hon, R., Weill, D.F. and Henry, D.J., 1980. Thermochemistry of glasses and liquids in the systems $CaMgSi_2O_6$–$CaAl_2Si_2O_8$–$NaAlSi_3O_8$, $CaAl_2Si_2O_8$–$NaAlSi_3O_8$ and SiO_2–Al_2O_3–CaO–Na_2O. *Geochim. Cosmochim. Acta* **44**, pp. 1409–1423.

Nekvasil, H. and Burnham, C.W., 1987. The calculated individual effects of pressure and water content on phase equilibria in the granite system. In: Mysen, B.O., Editor, , 1987. *Magmatic Processes: Physicochemical Principles*, The Geochemical Society, Pennsylvania, pp. 433–445.

Nicholls, J., 1980. A simple thermodynamic model for estimating the solubility of H_2O in magmas. *Contrib. Mineral. Petrol.* **74**, pp. 211–220.

Ochs, F.A.I. and Lange, R.A., 1997. The partial molar volume, thermal expansivity, and compressibility of H_2O in $NaAlSi_3O_8$ liquid: new measurements and an internally consistent model. *Contrib. Mineral. Petrol.* **129**, pp. 155–165.

Pichavant, M., Holtz, F. and McMillan, P., 1992. Phase relations and compositional dependence of H_2O solubility in quartz–feldspar melts. *Chem. Geol.* **96**, pp. 303–319.

Powell, R. and Holland, T., 1993. The applicability of least squares in the extraction of thermodynamic data from experimentally bracketed mineral equilibria. *Am. Mineral.* **78**, pp. 107–112.

Richet, P., 1987. Heat capacity of silicate glasses. *Chem. Geol.* **62**, pp. 111–127.

Richet, P. and Bottinga, Y., 1984. Glass transitions and thermodynamic properties of amorphous SiO_2, $NaAlSi_nO_{(2n+2)}$ and $KAlSi_3O_8$. *Geochim. Cosmochim. Acta* **48**, pp. 453–470.

Richet, P. and Bottinga, Y., 1986. Thermochemical properties of silicate glasses and liquids: a review. *Rev. Geophys.* **24**, pp. 1–25.

Richet, P. and Polian, A., 1998. Water as a dense icelike component in silicate glasses. *Science* **281**, pp. 396–398.

Salje, E., 1985. Thermodynamics of soldium feldspar: II. Experimental results and numerical calculations. *Phys. Chem. Miner.* **12**, pp. 99–107.

Shaw, H.R., 1964. Theoretical solubility of H_2O in silicate melts — quasi-crystalline models. *J. Geol.* **72**, pp. 601–617.

Shen, A. and Keppler, H., 1997. Direct observation of complete miscibility in the albite–H_2O system. *Nature* **385**, pp. 710–712.

Steiner, J.C., 1970. An experimental study of the assemblage alkali feldspar+liquid+quartz in the system $NaAlSi_3O_8$–$KAlSi_3O_8$–SiO_2–H_2O at 4000 bars. PhD dissertation, Stanford University, 98 pp.

Tuttle, O.F. and Bowen, N.L., 1958. Origin of granite in the light of experimental studies in the system $NaAlSi_3O_8$–$KAlSi_3O_8$–SiO_2–H_2O. *Geol. Soc. Am. Bull.* **74** 145 pp.

Wen, S. and Nekvasil, H., 1994. Ideal associated solutions: application to the system albite–quartz–H_2O. *Am. Mineral.* **79**, pp. 316–331.